FOSSIL IMPRINT • vol. 80 • 2024 • no. 1 • pp. 135–153

NATIONAL MUSEUM

LOWER DEVONIAN *TORTILICAULIS* IS AN EARLY TRACHEOPHYTE AND NOT A BRYOPHYTE

JENNIFER L. MORRIS[1,2], DIANNE EDWARDS[2,*], LINDSEY AXE[2], TOM CROOKS[1], DUNCAN MURDOCK[3], PHILIP C. J. DONOGHUE[1]

[1] Bristol Palaeobiology Group, School of Earth Sciences, University of Bristol, Life Sciences Building, 24 Tyndall Avenue, Bristol, BS8 1TQ, United Kingdom.
[2] School of Earth and Environmental Sciences, Cardiff University, Main Building, Park Place, Cardiff, CF10 3AT, United Kingdom; e-mail: EdwardsD2@cardiff.ac.uk.
[3] Oxford University Museum of Natural History, Parks Road, Oxford, OX1 3PW, United Kingdom.
[*] corresponding author

Morris, J. L., Edwards, D., Axe, L., Crooks, T., Murdock, D., Donoghue, P. C. J. (2024): Lower Devonian *Tortilicaulis* is an early tracheophyte and not a bryophyte. – Fossil Imprint, 80(1): 135–153, Praha. ISSN 2533-4050 (print), ISSN 2533-4069 (on-line).

Abstract: *Tortilicaulis* D.Edwards is a genus of long-standing unknown affinity in which there are two species: the holotype *T. transwalliensis* D.Edwards, known only from coalified compressions and *T. offaeus* D.Edwards, Fanning et J.B.Richardson, known from an assemblage of minute, exceptionally well preserved charcoalified fossils from a Lochkovian deposit in the Welsh Borderland. It has previously been interpreted as bryophyte-like after comparisons based on twisted cells in both stems and sporangia were made with certain extant liverwort and moss genera, there being no evidence of vascular tissues. It has previously been grouped within the horneophytes in cladistic analyses. Subsequent studies of *T. offaeus* confirmed the presence of stomata on their isotomously branching stems and dehiscence of the sporangium into two valves, but the absence or presence of tracheids has not been demonstrated. Despite numerous attempts to observe the internal anatomy of stems through physical splitting followed by scanning microscopy, we turned to synchrotron radiation x-ray tomography microscopy. Here we describe five *Tortilicaulis* specimens that were selected for scanning and demonstrate simple annular tracheids within their twisted stems. We conclude that *Tortilicaulis* was an early diverging tracheophyte, although whether a member of the stem or crown group awaits further detailed cladistic analyses. While architecturally similar to *Psilophyton* Dawson, the hypothesis that *Tortilicaulis* was ancestral to the trimerophytes remains unproven.

Key words: early tracheophytes, Lower Devonian, embryophytes, *Tortilicaulis*, tracheids, water-conducting cells, scanning electron microscopy, synchrotron radiation x-ray tomography microscopy, mesofossils

Received: August 9, 2024 | Accepted: October 8, 2024 | Issued: November 18, 2024

Introduction

The evolution of vascular tissues was a fundamental adaptation that led to the successful proliferation of plants on land. The development and specialisation of transport systems for fluids and nutrients (xylem and phloem), especially in the sporophyte generation, allowed early land plants to radiate into drier environments and to achieve larger body sizes. The presence of tracheary elements in stems is a primary synapomorphy for the tracheophytes; they are not present in bryophytes, although some mosses and liverworts do possess other types of water-conducting cells (Ligrone et al. 2000). The characterisation of the internal anatomy and nature of water-conducting cells within fossilised stems of known taxa is critical to the determination of their affinity.

Elucidating the stem anatomy of early embryophyte fossils is key to understanding the early evolutionary history and phylogenetic relationships between the major basal land plant lineages. There are many topologies hypothesised, including those resulting from molecular analysis (e.g., Qiu et al. 2006, Cox et al. 2014, Wickett et al. 2014). Recent phylogenomic analyses have found strong support for a liverwort-moss clade (Setaphyta) and bryophyte monophyly is favoured statistically over all competing topologies (Puttick et al. 2018, Sousa et al. 2019, One Thousand Plant Genomes Initiative 2019, Harris et al. 2020, 2022, Su et al. 2021). This topology has implications for understanding the ancestral state of the early embryophytes, namely that the ancestral embryophyte was likely more complex and tracheophyte-like than has previously been considered (Donoghue et al. 2021). Further confirmation of these results requires a total-evidence approach that directly incorporates fossil record data and thus demands a rigorous interrogation of early embryophytes from the fossil record.

DOI 10.37520/fi.2024.012

Much of our understanding of the stem anatomy and the water-conducting cells of early land plants comes from exceptionally preserved specimens from fossil Lagerstätten deposits, where permineralisation has allowed for the three-dimensional preservation of tissues at a cellular level, e.g., Rhynie chert plant fossils (first described by Kidston and Lang 1917; for a review see Kerp 2017); pyritized axes from the Brecon Beacons, Wales (Kenrick and Edwards 1988, Kenrick et al. 1991). Fossilised vascular tissues within stems are commonly determined by the presence of annular or helical secondary thickenings of elongate internal cells, which are analogous to tracheids within the protoxylem of extant vascular plants (Kenrick and Crane 1991, Edwards 1993, 2003). Where present, tracheid architecture (the delimitation of C, G, P and S-type tracheids) has also been an important character in differentiating between lineages of early tracheophytes (Kenrick and Crane 1991, 1997, Edwards 2003).

The first evidence of simple, annular secondary thickenings comes from the Late Silurian (Ludlow) within simply branching, naked stems terminated by *Cooksonia*-type sporangia (Edwards and Davies 1976). The tracheophytic affinity of this genus was confirmed by the presence of tracheids within a charcoalified *Cooksonia pertoni* W.H.Lang specimen from a Lower Devonian (Lochkovian) charcoal Lagerstätte from the Welsh Borderland, UK (Edwards et al. 1992).

This deposit has been prolific in yielding exceptionally preserved vegetative remains, including the cellular details of sporangia, in situ spores and branching stems, including stomata (e.g., Edwards 1996, 2000, Wellman et al. 1998, Edwards et al. 2014, 2021a, Morris et al. 2018). Charcoalification and the partial permineralisation by pyrite crystals has allowed for some three-dimensional preservation, but they have also been subjected to varying degrees of shrinkage and compression (Edwards and Axe 2004). This assemblage of minute fossils has provided significant insights into a hidden diversity of early embryophytes, including early tracheophytes (e.g., Edwards et al. 1994, Habgood et al. 2002, Morris et al. 2012) and the eophytes (Edwards et al. 2021b). The eophytes are a group of small, naked and bifurcating stems with occasional stomata that terminate in sporangia containing either permanent dyads or tetrads (Edwards et al. 2012). Water-conducting cells are not found within their stems, but elongate cells with thickenings similar to those in modern bryophytes are present.

Other types of water-conducting cells without secondary thickenings have been observed in isolated, naked stems from the same locality (Edwards and Axe 2000, Edwards et al. 2003), but frustratingly the severance of the terminal sporangia precludes their assignment to established taxa. Similar non-tracheal cells have been described from exceptional silicate permineralisations of *Aglaophyton* D.S.Edwards (Edwards 1986) and *Nothia* A.G.Lyon (Kerp et al. 2001) stems from the late Pragian – early Emsian Rhynie chert, Scotland. In both cases these cells are comparable to the water-conducting cells of some extant liverworts and mosses and highlights the 'hidden diversity' of water-conducting cells within seemingly identical smooth, naked stems.

It is in this context that we re-consider *Tortilicaulis* (Edwards 1979), a taxon that has been cited as of uncertain affinity or as bryophyte-like due to similar characteristics with certain extant genera of liverworts and mosses. However, without prior evidence of the internal anatomy of its smooth, naked stems, its affinity could not be resolved. In the cladistic analysis of Kenrick and Crane (1997), *Tortilicaulis* resolves as a member of the horneophytes, the earliest-diverging group of polysporangiophytes within the tracheophyte stem-group, a sister group to crown-

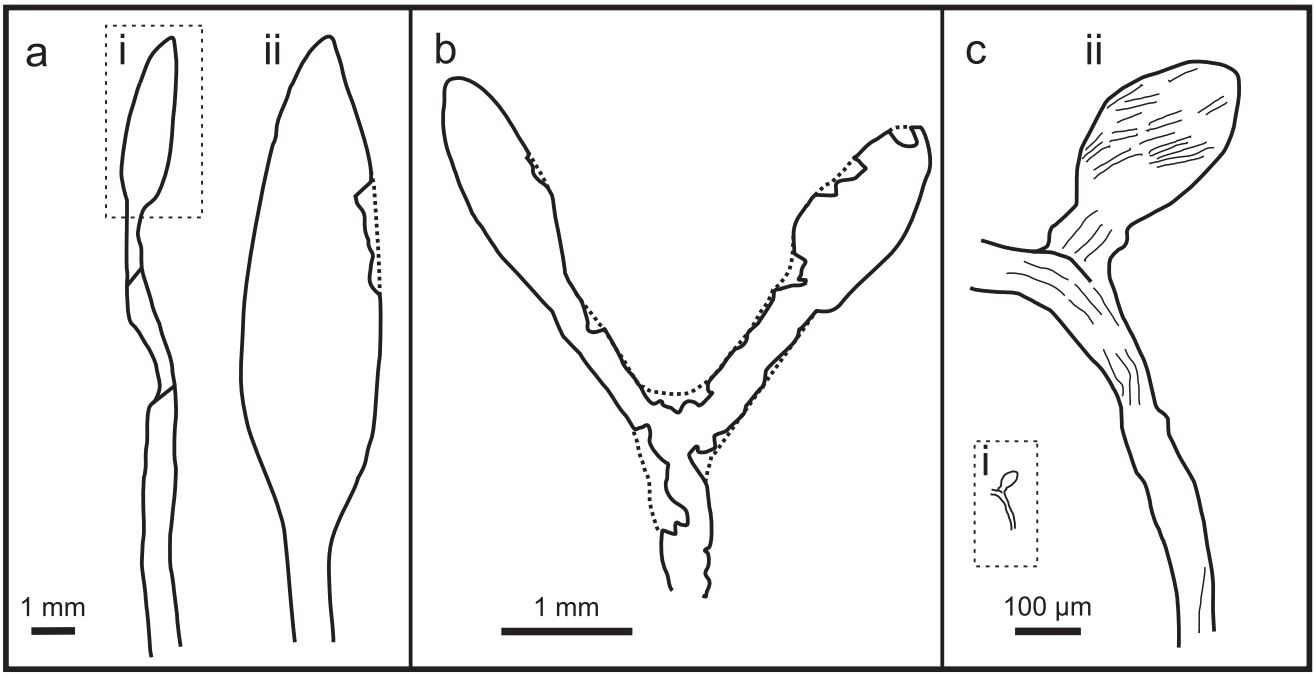

Text-fig. 1. Line drawings of the two species of *Tortilicaulis*. a: *Tortilicaulis transwalliensis* holotype. i) Whole specimen, ii) Close up of sporangium, scaled to specimen in (b). b: *T. transwalliensis*. Terminal sporangia attached to branching axis. c: *T. offaeus*. i) Specimen scaled to *T. transwalliensis* in (a, ii) and (b). ii) Magnification of the specimen, showing twisted cells.

tracheophytes (eutracheophytes). Here we present the first unequivocal evidence for vascular tissues in *Tortilicaulis offaeus* stems, in the form of elongate cells with secondary thickenings, using synchrotron radiation x-ray tomography microscopy (SRXTM; Donoghue et al. 2006). Using this new information, together with additional observations of *Tortilicaulis offaeus* since the species was first erected, we discuss a possible taxonomic and evolutionary position.

Previous studies of *Tortilicaulis*

The genus *Tortilicaulis* was first erected for coalified compression fossils collected from an Upper Silurian (Přídolí) coastal locality at Freshwater East Bay, Pembrokeshire, south-west Wales (Edwards 1979). The type species, *Tortilicaulis transwalliensis*, possessed elongate sporangia, fusiform to oval in shape, that terminated short, narrow (0.1–0.4 mm wide), and unbranched stems (Text-fig. 1a). Both stem and sporangia displayed twisting, the latter sometimes constricted at the junction. Removal of coalified material from sporangia revealed obliquely running striations beneath, interpreted as spirally-orientated cells. Discussions on affinities were limited by the absence of anatomy, but Edwards noted that the curvature and twisting of the subtending stems suggested that they once lacked rigidity and they bore similar morphological variations as recorded in the possible bryophyte fossil taxon *Sporogonites* T.Halle (Halle 1916, Andrews 1958). Further comparisons were made with sporophytes of *Pellia* Raddi, a jungermannialean liverwort, where the seta is twisted and ephemeral, lacking thickened cell walls and a cuticle.

The lack of evidence for vascular tissues in these *Tortilicaulis* stems could not rule out a tracheophyte affinity, as tracheids are rarely preserved in similar compression fossils, such as *Cooksonia* specimens from the same locality (Edwards 1979). Nevertheless, *Tortilicaulis* has been cited as 'non-vascular' or as evidence for bryophytes in the Upper Silurian (e.g., Pant and Bhowmik 1998, Yang et al. 2004, Ligrone et al. 2012, Banerjee and Dutta 2014). Comparisons have also been made to the sporophyte of the moss *Takakia* Hattori et Inoue, that is superficially similar in sporangial shape and spiralling sporangial and stem wall cells (Renzaglia et al. 1997, Jia et al. 2003). However, unlike *Tortilicaulis*, *Takakia* sporophytes possess a columella, calyptra and unbranched stems. In addition, the discovery of isotomous branching and in situ trilete monad spores in compression fossils assigned to *T. transwalliensis* from a younger, lower Lochkovian locality (Targrove Quarry, near Ludlow, UK) (Text-fig. 1b) rules out such affinity (Fanning et al. 1992).

Similar branching and trilete spores were also recorded in a second, but smaller species, *T. offaeus* (Text-fig. 1c), based on specimens from the middle Lochkovian charcoalified Lagerstätte of the Welsh Borderland, UK (Edwards et al. 1994). They were placed in the genus because the terminal sporangia showed similar variation in sporangial shape (although also include examples of bifurcating sporangia) and the presence of twisted cells in both the latter and the subtending stems. However, these three-dimensionally preserved fossils are much smaller than the type (stems 0.06–0.14 mm wide), and when analysed under SEM provided further details on the in situ spores and superficial cells of both sporangia and stems, including possible stomata. These differences justified erection of a new species. Unequivocal stomata were difficult to distinguish because shrinkage of elongate epidermal cells had obliterated any detail. Their position was marked by vertically elongate slits surrounded by flattened areas, but no obvious guard cells (Edwards et al. 1994: fig. 36). A straight unbranched sterile axis with identical surface features but lacking twisting when fractured showed what may have been a more deeply seated guard cell (Edwards et al. 1994: fig. 39, position arrowed in fig. 37).

Subsequent studies of numerous *Tortilicaulis offaeus* specimens have provided more conclusive evidence for stomata, such as specimen NMW 99.11G.1 (Pl. 1, Figs 1–6). In Pl. 1, Fig. 5, a stoma with collapsed guard cells surrounding a central pore can be seen. There is also further evidence for dehiscence of the sporangia into two valves, such as illustrated in Pl. 1, Fig. 8. Morris et al. (2012) illustrated of a complete sporangium where two rows of elongate cells appeared to be modified prior to splitting (Morris et al. 2012: pl. XIII, fig. 12).

Regarding the in situ spores, they are similar in appearance to those of the type species, but are much smaller (15–19 μm compared with 43–49 μm; Edwards et al. 1994: fig. 51). In both species, the very distinctive and abundant retusoid trilete in situ spores are covered with minute microconi and micrograna on both distal and proximal surfaces. They were assigned to the dispersed taxon, *Apiculiretusispora* sp., although the proximal surfaces of spores in this genus are typically laevigate. Via transmission electron microscopy (TEM), the spores within *T. offaeus* were found to possess tri-layered walls, with an electron-dense outer layer consisting of sculptural elements that are fully incorporated into the spore wall (Morris et al. 2012).

The stomatiferous bifurcating stems and trilete spores point to homoiohydry and some evidence for tracheophyte affinity, but repeated attempts to find unequivocal tracheids by fracturing the charcoalified remains have been unproductive. Horizontal intracellular structures have been observed in some superficial cells (Pl. 1, Fig. 6; Edwards et al. 1994: figs 40–43), but are thought to represent residual cytoplasm following charring (Edwards and Axe 2004). Therefore, to further investigate the internal structures, a selection of *T. offaeus* specimens was chosen for advanced visualisation using synchrotron radiation x-ray tomography microscopy (SRXTM).

A new approach

While progress has been made, one of the main frustrations working with the specimens from the Lochkovian charcoalified Lagerstätte of the Welsh Borderland is that they are very fragmentary, the majority being isolated axes with no indication of affinity (Morris et al. 2018, Edwards et al. 2021a). Where stems are attached to sporangia, they are usually too short to provide much information. As such, for many of the taxa from this assemblage, the inner stem anatomy has mostly eluded us. We primarily rely on natural fractures in the stem to observe internal structures under scanning electron microscopy (SEM), such as illustrated in Pl. 1, Fig. 7, with

some serendipitous discoveries (e.g., tracheids in *Cooksonia*; Edwards et al. 1992). The fragile nature of these minute axes leads to easy disintegration, and we have had variable results in attempts at physically dissecting the stems. Embedding and sectioning with a diamond knife to produce semi-thin sections has proved to be a useful technique, particularly for sporangia and spores (Morris et al. 2011, 2012), but this process is laborious, particularly with such small specimens, and ultimately destroys the specimen. Therefore, we turned to SRXTM, a technique that provides high resolution X-ray tomographic datasets for the visualisation, digital sectioning and reconstruction of both plant and animal fossils, without invasive or destructive preparation (Donoghue et al. 2006, Stampanoni et al. 2006, Friis et al. 2014). The appropriateness of this technique for the visualisation of not only fossil plants but specifically charcoalified mesofossils has been emphasised by the successful and informative tomographic datasets produced from three-dimensionally preserved Carboniferous fertile organs of seed ferns (Scott et al. 2009) and Cretaceous reproductive structures (flowers) (Friis et al. 2007, 2014) that have greatly enhanced the understanding of pteridosperm and early angiosperm evolution respectively. Through this technique it has been possible to dissect digitally a *Tortilicaulis offaeus* specimen with a branching stem, revealing the internal anatomy.

Material and methods

Specimens of *Tortilicaulis offaeus* were extracted from a grey siltstone horizon exposed in a stream section on the north side of Brown Clee Hill, in the Welsh Borderland, UK (Edwards et al. 1994). This bed is part of a sequence of siltstones, sandstones and calcretes assigned to the Freshwater West Formation (previously known as the St. Maughans Formation) of the Lower Old Red Sandstone, within the Anglo-Welsh Basin (Barclay et al. 2015). Palynological assemblages from this horizon were studied by John Richardson and assigned to the middle sub-zone of the *micrornatus-newportensis* Sporomorph Assemblage Biozone of Richardson and McGregor (1986), which indicates an early to middle Lochkovian age.

Two specimens were extracted from rocks collected from the site in 1995 (HD248/03 and HD270/01) and the remaining three specimens from a later collection in 2012 (HD743/01, HD(L)138/05 and HD(L)138/06). The specimens were treated the same way, extracted from the siltstone by disaggregation in water followed by standard HCl/HF maceration. They were recovered via sieving and left to air-dry, followed by screening and picking under a stereo light microscope (for further details on material preparation from this Lagerstätte, see earlier studies Edwards 1996, Morris et al. 2011). Promising specimens were then transferred to SEM stub, attached via sticky carbon disk, and coated in gold-palladium for examination under SEM (FEI ESEM-FEG). Five specimens identified as *Tortilicaulis offaeus*, were selected for SRXTM based on superficial morphology alone (e.g., spirally-orientated sporangial wall cells (Figs 1 in Pls 1–3, 5, 6), on the level of preservation, including the completeness of the specimen (sporangia with sufficient lengths of subtending stems), on the degree of three-dimensionality and on the lack of significant quantities of visible pyrite impregnation. These crystals can cause streak artefacts due to their high levels of x-ray absorption compared to charcoal. The specimens did not need any further processing for SRXTM but were carefully removed from the SEM stubs where they had been flat and were transferred on to brass pins (3 mm in diameter) and fixed in a vertical orientation by applying clear nail varnish at the base. This allows for maximum coverage of the specimen within the field-of-view and reduces the amount of contact between the specimen and the fixative, which aids in post-scan reconstruction.

Specimens were scanned at the TOMCAT X02DA beamline at the Swiss Light Source (SLS), Paul Scherrer Institut, Villigen, Switzerland (Stampanoni et al. 2006). Projections were obtained with beam energies of 10–23 KeV, exposures of 110–550 ms, using a 20 µm thick LAG:Ce or 5.9 µm thick LSO:Tb scintillator, 10×, 20× and 40× objectives, achieving voxel dimensions of 0.65 µm, 0.325 µm and 0.1625 µm, respectively. In each experiment, 1501 projections were acquired equi-angularly over 180° rotation within the beam. Projections were post-processed and rearranged into flat- and dark-field-corrected sinograms, and reconstruction was performed on a 60-core Linus PC farm, using a highly optimized routine based on the Fourier transform method and a regridding procedure (Marone et al. 2017). Slice data were analyzed using AVIZO 8.0 (www.thermofisher.com/avizo/software).

Results

Specimen HD248/03

Scanning electron microscopy

This specimen is a complete sporangium with a very short subtending stem (Pl. 2, Fig. 1). Where the stem is parallel-sided, it is 0.11 mm in diameter but widens into the base of the sporangium. The sporangium is 0.96 mm in total length and 0.37 mm wide at its widest point. It is fusiform in shape, with a rounded tip. A prominent longitudinal crack runs through the length of the sporangium, with several other small transverse cracks cutting across epidermal cells, indicating these are of taphonomic origin. Through most of the body, sporangial epidermal cells are elongate, with either a fusiform or columnar shape, and are typically between 15–20 µm in width. Cells at the tip become more equal in diameter, with a diamond shape appearance. The sporangial cells are twisted at angle of 30° from the long axis. As the cells taper into the subtending stem the angle of twisting reduces, and cells become more compressed, such that represented by elongate ridges.

SRXTM scans

The image in Pl. 2, Figs 2, 3 are slices through the whole of the specimen illustrated in Pl. 2, Fig. 1. The sporangium and parts of the stem have been permineralised with pyrite crystals (appearing bright white on the scans), such that much of the internal anatomy has been eliminated or damaged (e.g., in the base of sporangium, in the right side of the image it is filled with crystals, and where these have been chemically

etched away, the remaining cells have been destroyed, as arrowed (i) in Pl. 2, Fig. 4). The epidermal cells on one side of the sporangial wall have been preserved, as a single-cell thick wall approximately 35 µm in depth. These cells have thick outer periclinal walls (approximately 8–10 µm), and wedge-shaped anticlinal walls, tapering down into much narrower inner periclinal walls (approximately 1–2 µm). In some places, a second layer of cells are apparent between the outer epidermal cells and the sporangium content (arrowed in Pl. 2, Fig. 2). The 'cells' that fill the sporangium are interpreted as in situ spores. A higher resolution scan of the spores was not possible due to level of pyritization, and therefore the nature of the spore surfaces and ultrastructure could not be determined. However, the orientation of spores in relation to each other does provide useful information, such that separating tetrads of spores can be recognised, with at least three c-shaped spores clustered together, their proximal faces positioned towards each other.

The subtending stem (Pl. 2, Figs 4, 5) is also partially filled with pyrite crystals and cells are significantly compressed. There are rare occurrences of elongate cells that do not contain any crystals and have open internal spaces (arrowed in Pl. 2, Fig. 4) but no further detail of the cell ultrastructure or inner surface could be determined. There is a suggestion of thickenings along some surfaces (arrowed in Pl. 2, Fig. 5) but these are not conclusive.

Specimen HD270/01

Scanning electron microscopy

This specimen is a complete sporangium with a short length of subtending stem, with a branch point at the base (Pl. 3, Fig. 1). The sporangium is elongate, measuring approximately 0.76 mm in length and 0.44 mm at its widest point. It has a fusiform shape, gradually narrowing to a rounded tip. The sporangial epidermal cells exhibit the typical twisting, at an angle of around 40° from the longitudinal axis at the base. These cells are typically elongate, measuring around 55–80 µm in length and 10–17 µm in width, with tapering or columnar ends. Towards the sporangium tip, cells become shorter in length (ca. 30–40 µm) and twist more acutely (ca. 20°), some rectangular in shape, others more diamond-shaped where cell ends are tapered. Two prominent cracks run from the mid-point to the base of the sporangium (arrowed in Pl. 3, Fig. 1) and cut through the epidermal cells such that they are probably taphonomic in origin. The surface is occasionally covered with extraneous material. However, the sporangial wall remains intact such that its content is not visible.

The subtending stem is 430 µm in length between the base of the sporangium and the bifurcating branch point, widening slightly between 115 µm and 150 µm. As the fractured end of the stem on the left of the image in Pl. 3, Fig. 1 is wider (170 µm) than that on the right (150 µm), it would suggest that the latter is below the branch point. The angle of bifurcation is 144°. The epidermal cells of the stem have been compressed such that they are represented by elongate ridges and exhibit the same degree of twisting as the basal sporangium. The fractured end of the stem on the left of the image in Pl. 3, Fig 1 is figured in Pl. 3, Fig. 2 and shows some compression and pyritization but some internal cells had not collapsed and warranted further investigation.

SRXTM scans

The image in Pl. 3, Fig. 3 is a transverse slice through the sporangium, providing a section through the sporangial walls and revealing the content. The epidermal cells of the sporangial walls are partially preserved in places, with thick outer periclinal walls (approximately 7–15 µm) and wedge-shaped tapering anticlinal walls. Inner periclinal cell walls have mostly been destroyed but where present are thin (approximately 2 µm). The sporangium is partially filled with pyrite crystals particularly on one side but the remaining content is filled with compressed cells interpreted as in situ spores. Further details such as the nature of the spore surfaces could not be determined.

The images in Pl. 3, Figs 4–6 are longitudinal slices through the subtending stem. There are significant amounts of pyrite mineralisation that has caused some damage to internal stem anatomy, as well as interference on the scan, particularly evident in Pl. 3, Fig. 4. Where pyrite is not as prevalent, some internal stem anatomy has been partially preserved in the form of elongate cells (Pl. 3, Figs 5, 6). Occasional cell walls possess regularly spaced narrow thickenings (arrowed), but their presence or nature could not be clearly demonstrated.

Specimen HD743/01

Scanning electron microscopy

This specimen is a fragment of a smooth, naked stem with at least two dichotomies, possibly a third, terminated by elongate sporangia (Pl. 4, Figs 1–3). The branching angles are approximately 125°, giving the stem a bent appearance. Stem lengths between branch points are 1 mm, 0.65 mm and 0.42 mm, respectively from the base upwards, the final daughter branches being of equal length. The stem is more or less parallel-sided but narrows slightly after branching (0.16 mm after first dichotomy, 0.12 mm after final dichotomy). A series of elongate ridges runs along the length of the stem (Pl. 5, Fig. 1) and twist around its long axis to varying degrees, most prominently directly beneath the base of the sporangia (Pl. 4, Figs 2, 3). The ridges are interpreted as the remnants of epidermal axial cells, although it is not possible to demarcate the outlines of individual cells due to shrinkage, collapse and homogenisation of the cell walls during the charcoalification process (Edwards and Axe 2004). The outer surfaces of both stem and sporangia are covered with a thin and pustulous cuticular layer (Pl. 4, Fig. 4, Pl. 5, Fig. 3). The elongate ridges of the stem run continuously, apart from around depressions that contain a central pore. In some examples, these pores are surrounded by two poorly preserved, collapsed guard cells (Pl. 5, Fig. 3), thus are interpreted as stomata (see Pl. 4, Fig. 1 for their distribution, marked as dots). At the fractured, cross-sectioned ends of the stem, a zone of partially homogenised epidermal cells surrounds partially compressed internal tissue is observed (Pl. 5, Fig. 2).

The transition between the stem and the base of the sporangia is marked by a gradual widening and increase in the degree of twisting of the epidermal cells up to 45° from its long axis. The sporangia are fusiform in overall shape (Pl. 4, Figs 2, 3), taper to a rounded tip, each measuring

around 0.76 mm in length and 0.35 mm in maximum width (at approximately mid-height). Sporangial epidermal cells are elongate with tapering ends or are fusiform (Pl. 4, Figs 4, 5). In both sporangia, the wall is split in places, either across cells (fractures) or between cells. Exposed outer periclinal walls of the sporangial walls are around 15 µm in width. In the case of the latter, a row of cells with complete anticlinal walls lines the margin of the split (Pl. 4, Fig. 5) suggesting that this was a natural line of sporangial dehiscence. Although spores are mostly obscured, it can be determined that the in situ spores are separating tetrads and trilete monads with a distinctive sculpture (Pl. 4, Figs 6, 7). Trilete monads are approximately 20 µm in diameter. The distal surfaces are sculptured with densely packed microconi and micrograna that mostly occur as individuals but are fused in places. Where a proximal surface is visible, it is also ornamented with micrograna, including the triradiate fold (Pl. 4, Fig. 7), that are even smaller than those on the distal surfaces. This sculpture is typical of the in situ retusoid spores found within *T. offaeus* that has previously been assigned to *Apiculiretusispora* Streel (Edwards et al. 1994, Morris et al. 2012).

SRXTM

The image in Pl. 5, Fig. 4 is a longitudinal slice through the sporangium labelled (i) in Pl. 4, Fig. 1. The sporangial wall is a single-cell thick. The outer periclinal sporangial wall cells are thick (13–15 µm), with tapering anticlinal walls and thin inner periclinal walls (2 µm). There are in situ spores, the outline of some monads determinable but the nature of the spores could not be determined.

Longitudinal slices through the subtending stems are illustrated in Pl. 5, Figs 5–9. Although the stems are partially compressed and damaged by pyrite permineralisation in places, some of the internal anatomy has been preserved, with elongate cells that have internal voids. Some of these elongate cells possess regular internal thickenings that are approximately perpendicular to the long axes of the cells (arrowed in Pl. 5, Figs 5–9). Due to the twisted nature of the cells, it is a challenge to determine an accurate range of cell dimensions but they measure approximately between 40–120 µm in length and between 7.5–12.5 µm in width. The internal thickenings are approximately 1–1.7 µm in thickness and between 1.4 and 2.5 µm apart.

Specimen HD(L)138/05

Scanning electron microscopy

This specimen is a dichotomously branching stem but with only one daughter branch terminated by a sporangium (Pl. 6, Figs 1, 2). This is approximately 0.25 mm in length and 0.18 mm wide at maximum width. Compared to the other specimens discussed above, this sporangium is much smaller and has a lower length to width ratio (1.4, compared with between 1.7 to 2.6). It is fusiform with a tapering tip and sharply thins into parallel-sided subtending stem. The sporangial wall is partially damaged with fractures that cut across preserved sporangial cells (Pl. 6, Fig. 3). One fracture reveals the transverse section of the sporangial wall (arrow in Pl. 6, Fig. 3), approximately 8 µm thick. Sporangial cells are elongate and twisted by an angle of around 40° from the sporangial long axis. The sporangial cells are typically fusiform in shape, with tapering ends (Pl. 6, Fig. 3). Cells range between approximately 16 and 26 µm in length and between 7 and 12 µm in width.

The subtending stem is parallel-sided, approximately 0.55 µm in width and 0.68 mm in length before the branch point, beneath which is a further 0.32 mm of stem. Immediately beneath the sporangium, the outer periclinal walls of the epidermal cells are missing, such that the cells appear as elongate ridges (Pl. 6, Fig. 4) that twist around the long axis of the stem. Approximately 100 µm beneath the sporangium, a gap in these elongate ridges may represent a collapsed pore (arrow in Pl. 6, Fig. 2).

SRXTM

The images show in Pl. 6, Figs 5, 6 are longitudinal slices through the sporangium. In keeping with the specimens described above, the sporangial wall appears to be a single- or two cells thick, with thick outer periclinal walls (approximately between 5 and 15 µm) and thin inner periclinal walls (between 1 and 2 µm). The sporangium is filled with c shaped cells interpreted as in situ spores. In Pl. 6, Fig. 6, the proximal surface of single monad with a trilete mark is observed (arrowed). The resolution of the scans is insufficient to indicate detail of the distal surfaces, but a mottled appearance suggests that the surfaces are not smooth and bear some micro-sculpture. These in situ spores measure between 12 and 15 µm in total diameter.

Figs 8–11 in Pl. 6 are longitudinal slices through the subtending stem. There are partially permineralised with pyrite crystals and are compressed, but some elongate cells with open internal spaces are present. Due to the compression and twisting nature of the cells, the true length and nature of the cell endings are difficult to determine. These elongate cells possess regular internal thickenings that are approximately perpendicular to the long axes of the cells (arrowed in Pl. 6, Figs 9–11), but as with specimen HD270/01, their architecture cannot clearly be determined.

Specimen HD(L)138/06

Scanning electron microscopy

This specimen is a branching stem with one daughter branch terminated by a bifurcating sporangium (Pl. 7, Fig. 1). The stem is approximately 2.9 mm in total length, with the branch point 1.7 mm from the base of the specimen. The subtending stem is between 95 and 150 µm in width, and is tightly twisted, particularly in the basal part. The stem appears to gradually widen towards the proximal end, but not significantly, and is approximately parallel sided at the junction with the base of sporangium (Pl. 7, Fig. 2). Elongate ridges along the length of the stem are interpreted as compressed epidermal cells. These can be seen in transverse section of the fractured end of the daughter branch in Pl. 7, Fig. 3, forming a thick (ca. 9 µm) fused outer layer of the stem encompassing the internal anatomy of the stem. The elongate ridges are between 2 and 3.5 µm in height. Both the stem and the sporangium are partially covered with extraneous material (Pl. 7, Fig. 4).

The bifurcating sporangium is more complete on one side (right side of the image in Pl. 7, Fig. 2), measuring approximately 0.37 mm in length and 0.26 mm in width. It has a fusiform shape, gradually coming to a tip proximally. As illustrated in the specimens above, the sporangial epidermal cells are twisted around the long axis of the sporangium, at an angle of approximately 45°. The cells are elongate (between 23.5 and 45 µm in length and 9 and 12 µm in width), becoming more equal in dimensions towards the tip of the sporangium. Cells ends are either columnar or tapering. In places, the sporangial wall is fractured, cutting across cell boundaries. One such fracture reveals a limited view of the in situ spores. The visible spores are covered with a micro-sculpture on both the proximal and distal surfaces. A triradiate fold can be seen on the proximal surface of one spore (arrowed in Pl. 7, Fig. 5).

SRXTM

Longitudinal slices through the subtending stem (Pl. 7, Figs 6, 7) show that the stems are mostly compressed, apart from a few elongate cells with open internal spaces. One of these elongate cells have secondary internal thickenings (arrowed in Pl. 7, Figs 6, 7) that are regularly spaced. However no further information about the nature of these thickenings could be obtained.

Discussion

Determination of tracheids in *Tortilicaulis*

The SEM images and SXRTM scans of the *Tortilicaulis* specimens described here and in previous publications (Edwards et al. 1994, Edwards and Axe 2004) demonstrate the degrees of preservation that we observe in fossil plants from this assemblage. In particular, stem internal anatomy is so often compressed or damaged by mineralisation (pyrite crystals) or by charcoalification. In some specimens, natural fractures have revealed that within the intracellular spaces in some superficial elongate cells, irregular, narrow strands are seen and are attributed to degradation due to charring (Edwards et al. 1994, Edwards and Axe 2004). However, using SXRTM, we have been able to visualise cells that are more deeply seated and have revealed regularly spaced and consistent transverse thickenings of the inner walls of elongate cells that suggest they were indeed original structures and not artefacts of charcoalification (particularly evident in specimen HD743/01). The structures observed are interpreted as the true thickenings of a secondary wall, which are indicative of tracheids. They are similar in nature to the annular thickenings observed in the tracheids of other early land plants, e.g., *Cooksonia pertoni* (Edwards et al. 1992). This evidence strengthens the contention that *Tortilicaulis* is in fact an early tracheophyte, and not of bryophyte affinity.

Evolutionary position of *Tortilicaulis*

Although the discovery of tracheids confirms the tracheophyte status of *Tortilicaulis*, its position within the tracheophyte total-group and how it relates to other early tracheophytes remains uncertain, because of the lack of detailed ultrastructure of the tracheid architecture.

In 1968, Banks erected the subdivision Rhyniophytina to include the iconic genus, *Cooksonia* W.H.Lang, and the rest in the Rhyniaceae (Banks 1968, 1975). This classification was subsequently revised by Kenrick and Crane (1991, 1997) using cladistic analysis. In aiming to resolve the relationships between the basal lineages, they included within their 33 characters the following that were scored as unknown or absent for *Tortilicaulis*, that are now known to be present: stomata (present) tracheid thickenings (present), sporangium dehiscence (single, one sided). This analysis led to the creation of the polysporangiophytes (Kenrick and Crane 1991) to encompass the *Aglaophyton*, the horneophytes (e.g., *Horneophyton* Bargh.) and the tracheophytes. The tracheophytes (vascular plant total-group) were further subdivided into the eutracheophytes (the tracheophyte crown-group) and the rhyniophytes (e.g., *Rhynia* Kidst., *Huvenia* Hass). The rhyniophytes form a distinct group of early tracheophytes and include characters such as a distinctive type of sporangial abscission (Hass and Remy 1991) and S-type tracheids within water-conducting cells (Kenrick and Crane 1991, 1997). A group of polysporangiophytes with renalioid and cooksonioid sporangia (e.g., *Cooksonia*, *Uskiella* Shute et D.Edwards, *Renalia* Gensel) resolved as stem-group tracheophytes, some belonging to a basal sister group to the Lycophytina (group that include the zosterophylls and lycopsids), based on their sporangia with borders that dehisce into two valves.

In Kenrick and Crane's analysis, *Tortilicaulis* resolved as a member of the horneophytes, however, with new information it is more likely to have been an early diverging tracheophyte, although its position within the total-group is still unresolved. It is unlike the renalioid or cooksonioid taxa of the stem-group in sporangial shape and sporangial dehiscence. In possessing bivalved sporangia that are longer than wide, twisting associated with sporangial dehiscence, longitudinal dehiscence into two equal valves via modification of boundary cells (Morris et al. 2012), and with similar in situ spore types (*Apiculiretusispora* spp.), it was considered architecturally similar to *Psilophyton* by Gerrienne (1997). *Psilophyton* is characterised by three dimensional isotomously and anisotomously branching stems in which paired terminal sporangia are recurved. Despite the similarities in sporangial characteristics, this predominantly Emsian genus is characterised by P-type tracheids (with scalariform pitting), with *P. dawsonii* H.P.Banks possessing the most comprehensively described examples (Hartman and Banks 1980). A similar sporangial state is present in Emsian genus *Pertica* Kasper et H.N.Andrews (Kasper and Andrews 1972) but it lacks information on tracheids. Both *Psilophyton* and *Pertica* are considered to belong to the trimerophyte grade of plants, a paraphyletic group of basal euphyllophytes (Kenrick and Crane 1991, 1997). While Gerrienne (1997) hypothesised that plants with the organisation of *Tortilicaulis* were likely ancestral to the trimerophytes, information of such a relationship requires more information on tracheid ultrastructure than now available. The major uniting feature of the two genera is mode of sporangial dehiscence, a not infrequent method for spore dispersal in early land plants with elongate sporangia.

Acknowledgements

DE has greatly benefitted from the generous assistance of Cedric Shute, although saddened that our Sporogonites project was never completed. We thank Charles Wellman and Kate Habgood for the discovery and early identification of some specimens used in this study as part of their research activities at Cardiff University. This research has been supported by Leverhulme (RF-2002-167) and Gatsby grants, and NERC grant NE/J012610/1, which we gratefully acknowledge. We acknowledge the Paul Scherrer Institut, Villigen, Switzerland for provision of synchrotron radiation beamtime at the TOMCAT beamline X02DA of the SLS and would like to thank Federica Marone for assistance.

References

Andrews, H. N. (1958): Notes on Belgian specimens of *Sporogonites*. – The Palaeobotanist, 7: 85–89. https://doi.org/10.54991/jop.1958.573

Banks, H. P. (1968): The early history of land plants. – In: Drake, E. T. (ed.), Evolution and environment. New Haven, Yale University Press, pp. 73–107.

Banks, H. P. (1975): Early vascular land plants: proof and conjecture. – Biosciences, 25: 730–737. https://doi.org/10.2307/1297453

Banerjee, M., Dutta, S. (2014): First record of metzgeriinean bryophyte *Pantiathallites gondwanensis* gen. et. sp. nov. in the *Glossopteris* floral assemblage of late early Permian of India. – Proceedings of the National Academy of Sciences, India Section B: Biological Sciences, 84: 447–455. https://doi.org/10.1007/s40011-013-0225-3

Barclay, W. J., Davies, J. R., Hillier, R. D., Waters, R. A. (2015): Lithostratigraphy of the Old Red Sandstone successions of the Anglo-Welsh Basin (British Geological Survey Reports, Research reports, RR/14/002). – British Geological Survey, Keyworth, UK, 196 pp.

Cox, C. J., Li, B., Foster, P. G., Embley, T. M., Civán, P. (2014): Conflicting phylogenies for early land plants are caused by composition biases among synonymous substitutions. – Systematic Biology, 63: 272–279. https://doi.org/10.1093/sysbio/syt109

Donoghue, P. C. J., Bengtson, S., Dong, X.-P., Gostling, N. J., Huldtgren, T., Cunningham, J. A., Yin, C., Yue, Z., Peng, F., Stampanoni, M. (2006): Synchrotron X-ray tomographic microscopy of fossil embryos. – Nature, 442: 680–683. https://doi.org/10.1038/nature04890

Donoghue, P. C. J., Harrison, C. J., Paps, J., Schneider, H. (2021): The evolutionary emergence of land plants. – Current Biology, 31(19): R1281–R1298. https://doi.org/10.1016/j.cub.2021.07.038

Edwards, D. (1979): A late Silurian flora from the Lower Old Red Sandstone of south-west Dyfed. – Palaeontology, 22: 23–52.

Edwards, D. (1993): Cells and tissues in the vegetative sporophytes of early land plants. – New Phytologist, 125: 225–247. https://doi.org/10.1111/j.1469-8137.1993.tb03879.x

Edwards, D. (1996): New insights into early land ecosystems: A glimpse of a Lilliputian world. – Review of Palaeobotany and Palynology, 90: 159–174. https://doi.org/10.1016/0034-6667(95)00081-X

Edwards, D. (2000): The role of mid-Palaeozoic mesofossils in the detection of early bryophytes. – Philosophical Transactions of the Royal Society of London, B, 355: 733–755. https://doi.org/10.1098/rstb.2000.0613

Edwards, D. (2003): Xylem in early tracheophytes. – Plant, Cell and Environment, 26: 57–72. https://doi.org/10.1046/j.1365-3040.2003.00878.x

Edwards, D., Axe, L. (2000): Novel conducting tissues in Lower Devonian plants. – Botanical Journal of the Linnean Society, 134: 383–399. https://doi.org/10.1006/bojl.2000.0378

Edwards, D., Axe, L. (2004): Anatomical evidence in the detection of the earliest wildfires. – Palaios, 19: 113–128. https://doi.org/10.1669/0883-1351(2004)019<0113:AEITDO>2.0.CO;2

Edwards, D., Axe, L., Duckett, J. G. (2003): Diversity in conducting cells in early land plants comparison with extant bryophytes. – Botanical Journal of the Linnean Society, 141: 297–347. https://doi.org/10.1046/j.1095-8339.2003.00153.x

Edwards, D., Davies, E. C. W. (1976): Oldest recorded *in situ* tracheids. – Nature, 263: 494–495. https://doi.org/10.1038/263494a0

Edwards, D., Davies, K. L., Axe, L. (1992): A vascular conducting strand in the early land plant *Cooksonia*. – Nature, 357: 683–685. https://doi.org/10.1038/357683a0

Edwards, D., Fanning, U., Richardson, J. B. (1994): Lower Devonian coalified sporangia from Shropshire: *Salopella* Edwards & Richardson and *Tortilicaulis* Edwards. – Botanical Journal of the Linnean Society, 116: 89–110. https://doi.org/10.1111/j.1095-8339.1994.tb00425.x

Edwards, D., Morris, J. L., Axe, L., Duckett, J. G. (2021a): Picking up the pieces: New charcoalified plant mesofossils (eophytes) from a Lower Devonian Lagerstätte in the Welsh Borderland, UK. – Review of Palaeobotany and Palynology, 297: 104567 (32 pp.). https://doi.org/10.1016/j.revpalbo.2021.104567

Edwards, D., Morris, J. L., Axe, L., Duckett, J. G., Pressel, S., Kenrick, P. (2021b): Piecing together the eophytes – a new group of ancient plants containing cryptospores. – New Phytologist, 233: 1440–1455. https://doi.org/10.1111/nph.17703

Edwards, D., Morris, J. L., Richardson, J. B., Kenrick, P. (2014): Cryptospores and cryptophytes reveal hidden diversity in early land floras. – New Phytologist, 202: 50–78. https://doi.org/10.1111/nph.12645

Edwards, D., Richardson, J. B., Axe, L., Davies, K. L. (2012): A new group of Early Devonian plants with valvate sporangia containing sculptured permanent dyads. – Botanical Journal of the Linnean Society, 168: 229–257. https://doi.org/10.1111/j.1095-8339.2011.01207.x

Edwards, D. S. (1986): *Aglaophyton major*, a non-vascular land plant from the Devonian Rhynie Chert. – Botanical Journal of the Linnean Society, 93: 173–204. https://doi.org/10.1111/j.1095-8339.1986.tb01020.x

Fanning, U., Edwards, D., Richardson, J. B. (1992): A diverse assemblage of early land plants from the Lower Devonian of the Welsh Borderland. – Botanical Journal of the Linnean Society, 109: 161–188. https://doi.org/10.1111/j.1095-8339.1992.tb00264.x

Friis, E. M., Crane, P. R., Pedersen, K. R., Bengtson, S., Donoghue, P. C. J., Grimm, W., Stampanoni, M. (2007): Phase contrast enhanced synchrotron-radiation X-ray analyses of Cretaceous seeds link Gnetales to extinct Bennettitales. – Nature, 450: 549–552. https://doi.org/10.1038/nature06278

Friis, E. M., Marone, F., Pedersen, K. R., Crane, P. R., Stampanoni, M. (2014): Three-dimensional visualization of fossil flowers, fruits, seeds, and other plant remains using synchrotron radiation X-ray tomographic microscopy (SRXTM): New insights into Cretaceous plant diversity. – Journal of Paleontology, 88: 684–701. https://doi.org/10.1666/13-099

Gerrienne, P. (1997): The fossil plants from the Lower Devonian of Marchin (northern margin of Dinant Synclinorium, Belgium). V. *Psilophyton genseliae* sp. nov., with hypotheses on the origin of Trimerophytina. – Review of Palaeobotany and Palynology, 98: 303–324. https://doi.org/10.1016/S0034-6667(97)00010-9

Habgood, K. S., Edwards, D., Axe, L. (2002): New perspectives on *Cooksonia* from the Lower Devonian of the Welsh Borderland. – Botanical Journal of the Linnean Society, 129: 339–359. https://doi.org/10.1046/j.1095-8339.2002.00073.x

Halle, T. G. (1916): A fossil sporogonium from the Lower Devonian of Röragen in Norway. – Botaniska Notiser, 2: 79–81.

Harris, B. J., Clark, J. W., Schrempf, D., Szöllősi, G. J., Donoghue, P. C. J., Hetherington, A. M., Williams, T. A. (2022): Divergent evolutionary trajectories of bryophytes and tracheophytes from a complex common ancestor of land plants. – Nature Ecology & Evolution, 6: 1634–1643. https://doi.org/10.1038/s41559-022-01885-x

Harris, B. J., Harrison, C. J., Hetherington, A. M., Williams, T. A. (2020): Phylogenomic evidence for the monophyly of bryophytes and the reductive evolution of stomata. – Current Biology, 30: 2001–2012. https://doi.org/10.1016/j.cub.2020.03.048

Hartman, C. M., Banks, H. P. (1980): Pitting in *Psilophyton dawsonii*, an early Devonian trimerophyte. – American Journal of Botany, 67: 400–412. https://doi.org/10.1002/j.1537-2197.1980.tb07665.x

Hass, H., Remy, W. (1991): *Huvenia kleui* nov. gen., nov. spec.: ein Vertreter der Rhyniaceae aus dem Höheren Siegen des Rheinischen Schiefergebirges. – Argumenta Palaeobotanica, 8: 141–168.

Jia, Y., Wu, P.-C., Wang, M.-Z., He, S. (2003): Takakiopsida, a unique taxon of bryophytes. – Acta Phytotaxonomica Sinica, 41: 350–361. (in Chinese, with abstract in English)

Kasper, A. E., Andrews, H. N. (1972): *Pertica*, a new genus of Devonian plants from northern Maine. – American Journal of Botany, 61: 339–359. https://doi.org/10.2307/2441116

Kenrick, P., Crane, P. R. (1991): Water-conducting cells in early fossil land plants: Implications for the early evolution of tracheophytes. – Botanical Gazette, 152: 335–356. https://doi.org/10.1086/337897

Kenrick, P., Crane, P. R. (1997): The origin and early evolution of plants on land. – Nature, 389: 33–39. https://doi.org/10.1038/37918

Kenrick, P., Edwards, D. (1988): The anatomy of Lower Devonian *Gosslingia breconensis* Heard based on pyritized axes, with some comments on the permineralization process. – Botanical Journal of the Linnean Society, 97: 95–123. https://doi.org/10.1111/j.1095-8339.1988.tb02456.x

Kenrick, P., Edwards, D., Dales, R. C. (1991): Novel ultrastructure in water-conducting cells of the Lower Devonian plant *Sennicaulis hippocrepiformis*. – Palaeontology, 34: 751–766.

Kerp, H. (2017): Organs and tissues of Rhynie chert plants. – Philosophical Transactions of the Royal Society, B, 373: 20160495 (16 pp.). https://doi.org/10.1098/rstb.2016.0495

Kerp, H., Hass, H., Mosbrugger, V. (2001): New data on *Nothia aphylla* Lyon 1964 ex El- Saadawy et Lacey 1979, a poorly known plant from the Lower Devonian Rhynie Chert. – In: Gensel, P. G., Edwards, D. (eds), Plants Invade the Land: Evolutionary and Environmental Perspectives. Columbia University Press, New York, USA, pp. 52–82. https://doi.org/10.7312/gens11160-005

Kidston, R., Lang, W. H. (1917): On Old Red Sandstone plants showing structure, from the Rhynie chert bed, Aberdeenshire. Part I. *Rhynia Gwynne-vaughani* Kidston & Lang. –Transactions of the Royal Society of Edinburgh, 51: 761–784. https://doi.org/10.1017/S0080456800008991

Ligrone, R., Duckett, J. G., Renzaglia, K. (2000): Conducting tissues and phyletic relationships of bryophytes. – Philosophical Transactions of the Royal Society of London, B, 355: 705–813. https://doi.org/10.1098/rstb.2000.0616

Ligrone, R., Duckett, J. G., Renzaglia, K. (2012): Major transitions in the evolution of early land plants: A bryological perspective. – Annals of Botany, 109: 851–871. https://doi.org/10.1093/aob/mcs017

Marone, F., Studer, A., Billich, H., Sala, L., Stampanoni, M. (2017): Towards on-the-fly data post-processing for real-time tomographic imaging at TOMCAT. – Advances in Structural Chemistry Imaging, 3: 1 (11 pp.). https://doi.org/10.1186/s40679-016-0035-9

Morris, J. L., Edwards, D., Richardson, J. B. (2018): The advantages and frustrations of a plant Lagerstätte as illustrated by a new taxon from the Lower Devonian of the Welsh Borderland, UK. – In: Krings, M., Harper, C. J., Cuneo, N. R., Rothwell, G. W. (eds), Transformative paleobotany: Papers to commemorate the life and legacy of Thomas N. Taylor. Academic Press/Elsevier Inc., London, pp. 49–67. https://doi.org/10.1016/B978-0-12-813012-4.00004-8

Morris, J. L., Edwards, D., Richardson, J. B., Axe, L., Davies, K. L. (2011): New plant taxa from the Lower

Devonian (Lochkovian) of the Welsh Borderland, with a hypothesis on the relationship between hilate and trilete spore producers. – Review of Palaeobotany and Palynology, 167: 51–81. https://doi.org/10.1016/j.revpalbo.2011.06.007

Morris, J. L., Edwards, D., Richardson, J. B., Axe, L., Davies, K. L. (2012): Further insights into trilete spore producers from the Early Devonian (Lochkovian) of the Welsh Borderland, U.K. – Review of Palaeobotany and Palynology, 185: 35–63. https://doi.org/10.1016/j.revpalbo.2012.08.001

One Thousand Plant Transcriptomes Initiative (2019): One thousand plant transcriptomes and the phylogenomics of green plants. – Nature, 574: 679–685. https://doi.org/10.1038/s41586-019-1693-2

Pant, D. D., Bhowmik, N. (1998): Fossil bryophytes – with special reference to Gondwanaland forms. – In: Chopra, R. N. (ed.), Topics in Bryology. Allied Publishers, Mumbai, pp. 1–52.

Puttick, M. N., Morris, J. L., Williams, T. A., Cox, C. J., Edwards, D., Kenrick, P., Pressel, S., Wellman, C. H., Schneider, H., Pisani, D., Donoghue, P. C. J. (2018): The interrelationships of land plants and the nature of the ancestral embryophyte. – Current Biology, 28: 1–13. https://doi.org/10.1016/j.cub.2018.01.063

Qiu, Y.-L., Li, L., Wang, B., Chen, Z., Knoop, V., Groth-Malonek, M., Dombrovska, O., Lee, J., Kent, L., Rest, J., Estabrook, G. F., Hendry, T. A., Taylor, D. W., Testa, C. M., Ambros, M., Crandall-Stotler, B., Duff, R. J., Stech, M., Frey, W., Quandt, D., Davis, C. C. (2006): The deepest divergences in land plants inferred from phylogenomic evidence. – Proceedings of the National Academy of Sciences (PNAS), 103: 15511–15516. https://doi.org/10.1073/pnas.0603335103

Renzaglia, K., McFarland, K., Smith, D. (1997): Anatomy and ultrastructure of the sporophyte of *Takakia ceratophylla* (Bryophyta). – American Journal of Botany, 84: 1337–1350. https://doi.org/10.2307/2446132

Richardson, J. B., McGregor, D. C. (1986): Silurian and Devonian spore zones of the Old Red Sandstone Continent and adjacent regions. – Bulletin of the Geological Survey of Canada, 364: 1–79. https://doi.org/10.4095/120614

Stampanoni, M., Groso, A., Isenegger, A., Mikuljan, G., Chen, Q., Bertrand, A., Henein, S., Betemps, R., Frommherz, U., Böhler, P., Meister, D., Lange, M., Abela, R. (2006): Trends in synchrotron-based tomographic imaging: the SLS experience. – In: Bonse, U. (ed.), Developments in X-ray Tomography V. Proceedings of the Society of Photo-Optical Instrumentation Engineers (SPIE), 6318: 63180M (14 pp.) https://doi.org/10.1117/12.679497

Scott, A. C., Galtier, J., Gostling, N. J., Smith, S. Y., Collinson, M. E., Stampanoni, M., Marone, F., Donoghue, P. C. J., Bengtson, S. (2009): Scanning electron microscopy and synchrotron radiation X-ray tomographic microscopy of 330 million year old charcoalified seed fern fertile organs. – Microscopy and Microanalysis, 15: 166–173. https://doi.org/10.1017/S1431927609090126

Sousa, F., Foster, P. G., Donoghue, P. C. J., Schneider, H., Cox, C. J. (2019): Nuclear protein phylogenies support the monophyly of the three bryophyte groups (Bryophyta Schimp.). – New Phytologist, 222: 565–575. https://doi.org/10.1111/nph.15587

Su, D., Yang, L., Shi, X., Ma, X., Zhou, X., Hedges, S. B., Zhong, B. (2021): Large-scale phylogenomic analyses reveal the monophyly of bryophytes and Neoproterozoic origin of land plants. – Molecular Biology & Evolution, 38: 3332–3344. https://doi.org/10.1093/molbev/msab106

Wickett, N. J., Mirarab, S., Nguyen, N., Warnow, T., Carpenter, E., Matasci, N., Ayyampalayam, S., Barker, M. S., Burleigh, J. G., Gitzendanner, M. A., Ruhfel, B. R., Wafula, E., Der, J. P., Graham, S. W., Mathews, S., Melkonian, M., Soltis, D. E., Soltis, P. S., Miles, N. W., Rothfels, C. J., Pokorny, L., Shaw, A. J., DeGironimo, L., Stevenson, D. W., Surek, B., Villarreal, J. C., Roure, B., Philippe, H., dePamphilis, C. W., Chen, T., Deyholos, M. K., Baucom, R. S., Kutchan, T. M., Augustin, M. M., Wang, J., Zhang, Y., Tian, Z., Yan, Z., Wu, X., Sun, X., Wong, G. K., Leebens-Mack, J. (2014): Phylotranscriptomic analysis of the origin and early diversification of land plants. – Proceedings of the National Academy of Sciences (PNAS), 111(45): E4859–E4868. https://doi.org/10.1073/pnas.1323926111

Wellman, C. H., Edwards, D., Axe, L. (1998): Permanent dyads in sporangia and spore masses from the Lower Devonian of the Welsh Borderland. – Botanical Journal of the Linnean Society, 127: 117–147. https://doi.org/10.1111/j.1095-8339.1998.tb02092.x

Yang, R.-D., Mao, J.-R., Zhang, W.-H., Jiang, L.-J., Gao, H. (2004): Bryophyte-like fossils (*Parafunaria sinensis*) from Early-Middle Cambrian Kaili Formation in Guizhou Province, China. – Acta Botanica Sinica, 46: 180–185.

Explanations of the plate

PLATE 1

Tortilicaulis, specimen NNW.99.11G.1

1. SEM image of whole specimen. Scale bar = 500 µm.
2. Magnification of the stem at the most proximal fractured branch point, with a stoma visible in the daughter branch (arrowed). Scale bar = 50 µm.
3. Magnification of the most distal end of the specimen, illustrating the fractured end of the stem and stoma arrowed. Scale bar = 50 µm.
4. Magnification of the stoma that is arrowed shown in Fig. 2. Scale bar = 20 µm.
5. Magnification of stoma arrowed in Fig. 3. Two collapsed guard cells flank a central pore. Scale bar = 20 µm.
6. Section through the fractured end of the specimen, with a cell that has internal structures. Scale bar = 10 µm.

Tortilicaulis, specimen KH003/03

7. Fractured end of a *Tortilicaulis* stem with minimal compression. A thick outer layer of tissue surrounds internal anatomy with open spaces. Scale bar = 20 µm.

Tortilicaulis, specimen HD 190/05

8. Partially intact and empty sporangium of *Tortilicaulis*, with one valve missing. Edges of valve are smooth. Scale bar = 100 µm.

PLATE 2

Tortilicaulis, specimen HD248/03

1. SEM image of whole specimen; sporangium with short subtending stem. Scale bar = 200 µm.

2., 3. SRXTM images (projections taken at ×20 magnification, 23 kV), longitudinal slices of the whole specimen. Arrow in Fig. 2 indicating where second layer of cells occurs between the sporangial epidermal cells and in situ spores. Scale bars = 200 µm.

4. Close up of Fig. 2, magnified on the subtending stem. Arrow indicates single elongate cell that is less compressed that those surrounding cells, without pyrite crystals. No clear content can be determined. Scale bar = 50 µm.
5. Close up of Fig. 3, magnified on the subtending stem. Arrow indicates a suggestion of thickenings. Scale bar = 50 µm.

PLATE 3

Tortilicaulis, specimen HD270/01, SEM images

1. SEM image of the whole specimen; sporangium with subtending stem, with branch point at the base. Scale bar = 200 µm.
2. SEM image of the cross section of the subtending stem. Scale bar = 50 µm.

Tortilicaulis, specimen HD270/01, SRXTM images (projections taken at ×20 magnification, 13 kV)

3. Transverse section through the sporangium. Scale bar = 50 µm.
4. Longitudinal section through the subtending stem. Scale bar = 100 µm.
5. Longitudinal section through the subtending stem, with arrows indicating thickenings. Scale bar = 20 µm.
6. Longitudinal section through the subtending stem, with arrows indicating thickenings. Scale bar = 20 µm.

PLATE 4

Tortilicaulis, specimen HD743/01, SEM images

1. Whole specimen, dichotomously branching stem with two terminal sporangia (i and ii). Dots represent positions of stomata. Scale bar = 1 mm.
2. Magnification of sporangium (i). Scale bar = 200 µm.
3. Magnification of sporangium (ii). Scale bar = 200 µm.
4. Magnification of the tip of sporangium (ii). Scale bar = 100 µm.
5. Magnification of tip of sporangium (ii), showing split between epidermal cells, possibly a line of dehiscence, exposing the spores within. Note the completeness of the anticlinal walls of the cells that line the margin of the split. Scale bar = 50 µm.
6. View of the in situ spores revealed between the split in the sporangial wall. Scale bar = 10 µm.
7. Magnification of the spore distal surface (densely packed microconi) and proximal surface of the spore beneath, with triradial fold (arrowed) and surface covered with micrograna. Scale bar = 2 µm.

PLATE 5

Tortilicaulis, specimen HD743/01, SEM images of the subtending stem

1. Elongate ridges, interpreted as epidermal cells, running along the length of stem, partially covered with thin, pustulous cuticular layer. Note two depressions/pores, interpreted as stomata with two guard cells. Scale bar = 50 µm.
2. Fractured end of the subtending stem, below the most distal branch point. Scale bar = 20 µm.
3. Magnification of pore, with two poorly preserved, collapsed guard cells. Scale bar = 10 µm.

Tortilicaulis, specimen HD743/01, SRXTM images (projections taken at ×10 magnification, 10 kV)

4. Longitudinal slice through sporangium (i) as imaged in Pl. 3, Fig. 1. Scale bar = 200 µm.

5.–9. Longitudinal slices through the subtending stem. Arrows indicate elongate cells with regularly-spaced internal secondary thickenings. Scale bar = 100 µm.

PLATE 6

Tortilicaulis, specimen HD743/01, specimen HD(L)138/05, SEM images

1. SEM image of the whole specimen, branching stem with one branch remaining, terminated by a single sporangium. Scale bar = 200 µm.
2. SEM image of the sporangium in Fig. 1, terminating a twisted subtending stem. Possible pore indicated by arrow. Scale bar = 50 µm.
3. SEM image of the basal portion of the sporangium and subtending stem. Arrow indicates a transverse fracture through the sporangial wall. Scale bar = 50 µm.
4. SEM image showing tilted view of basal portion of the sporangium and subtending stem. Scale bar = 50 µm.

Tortilicaulis, specimen HD743/01, SRXTM images (projections taken at ×20 magnification, 14 kV)

5., 6. Longitudinal slices through the sporangium. Scale bars = 50 µm.

7. Transverse section through the sporangium wall and in situ spores. Arrow indicates spore with trilete mark. Scale bar = 20 µm.

8.–11. Longitudinal sections through the subtending stem. Arrows indicate elongate cells with internal secondary thickenings. Scale bars = 20 µm.

PLATE 7

Tortilicaulis, specimen HD(L)138/06

1. SEM image of whole specimen, branching stem terminated by a bifurcating sporangium. Scale bar = 500 µm.
2. SEM image of subtending stem with view of the base of the bifurcating sporangium. Scale bar = 200 µm.
3. SEM image of the fractured end of the daughter branch of subtending stem, transverse section. Scale bar = 20 µm.
4. SEM image of the tip of one side of the sporangium, covered with extraneous material. Scale bar = 50 µm.
5. SEM image of the in situ spores, with one proximal surface visible, with a triradiate fold. Scale bar = 5 µm.

6., 7. SRXTM images (projections taken at ×20 magnification, 14 kV). Longitudinal slices through the subtending stem. Scale bar = 50 µm.

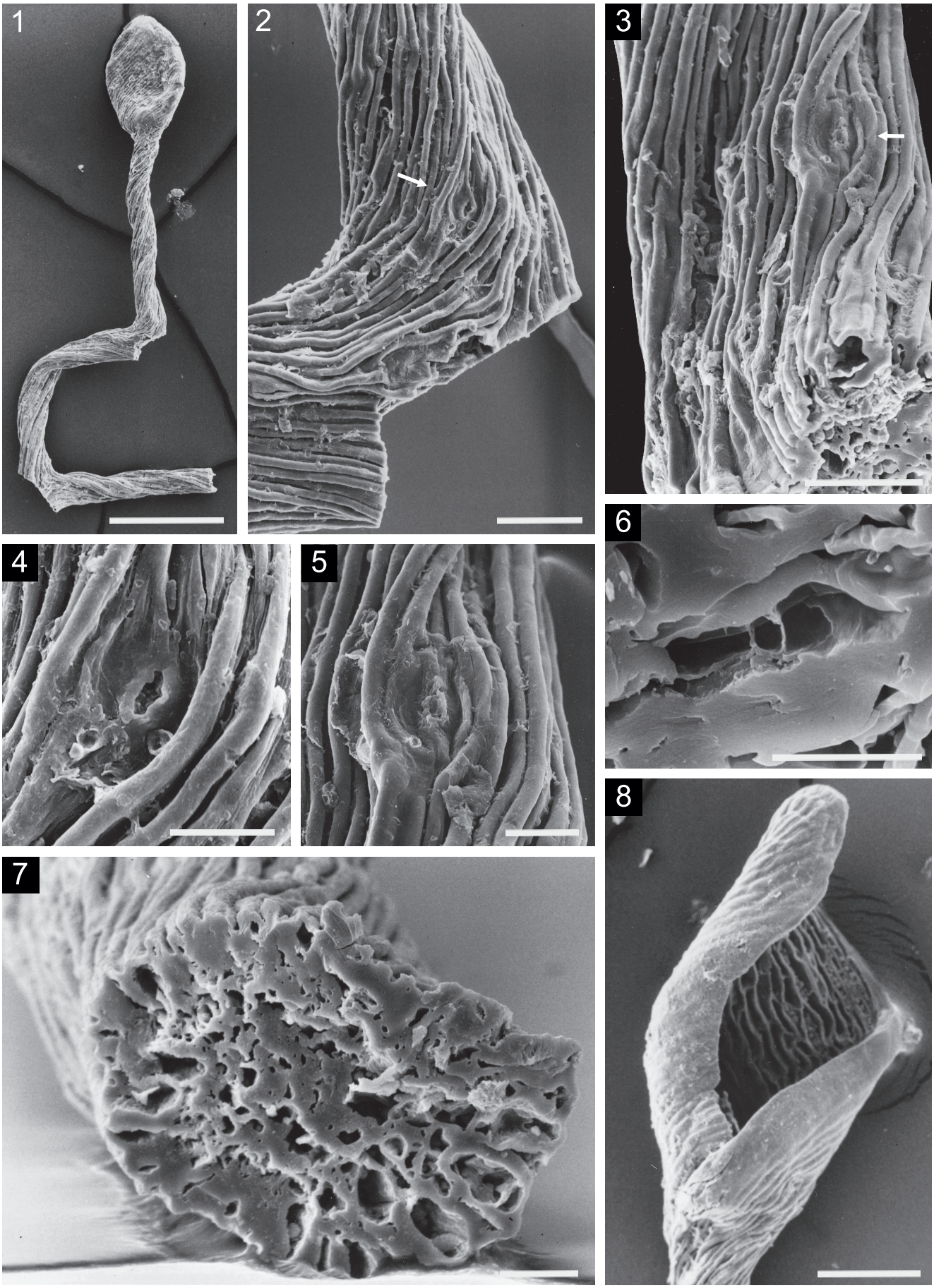
1
2
3
4
5
6
7
8

PLATE 2

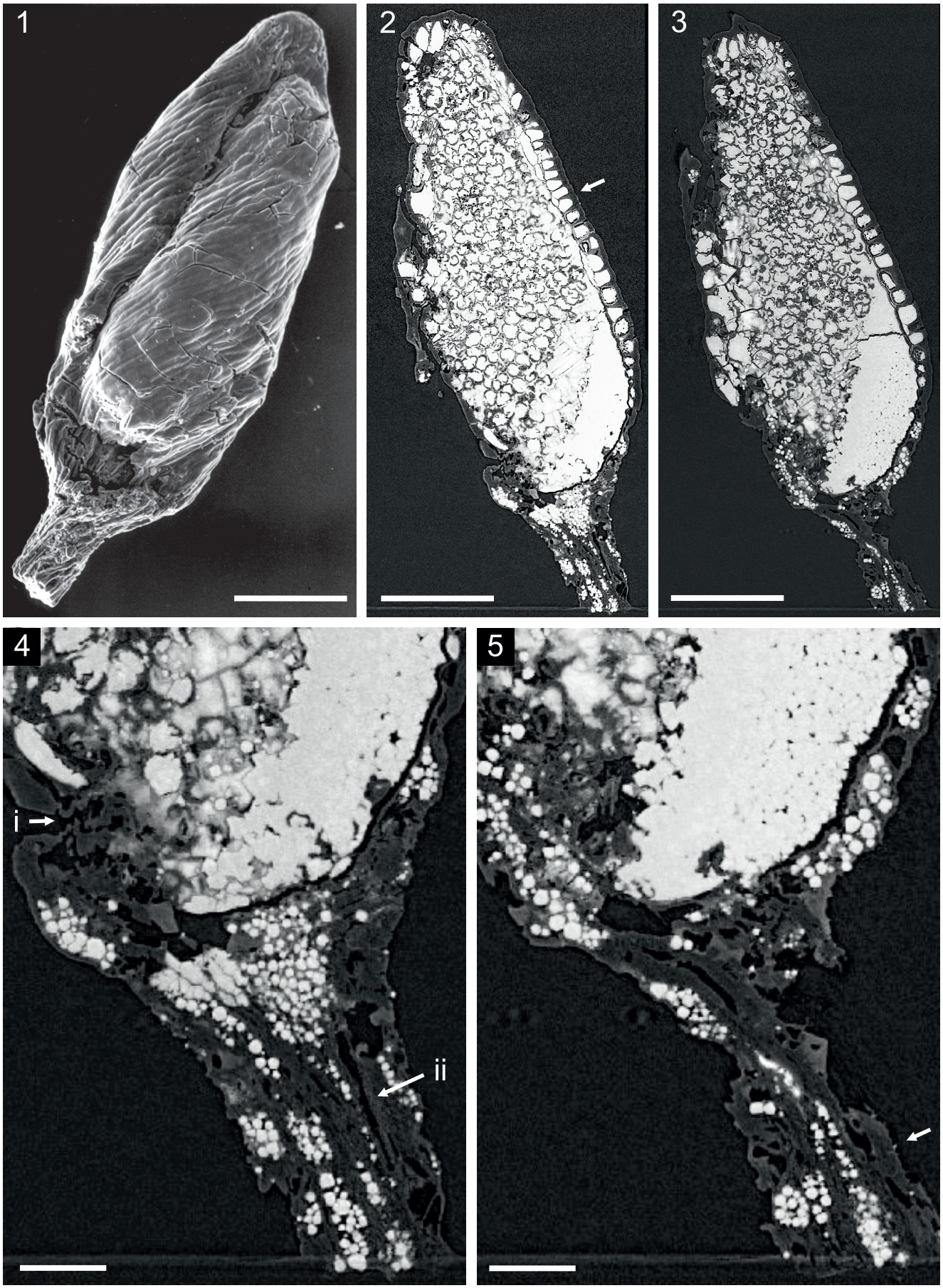

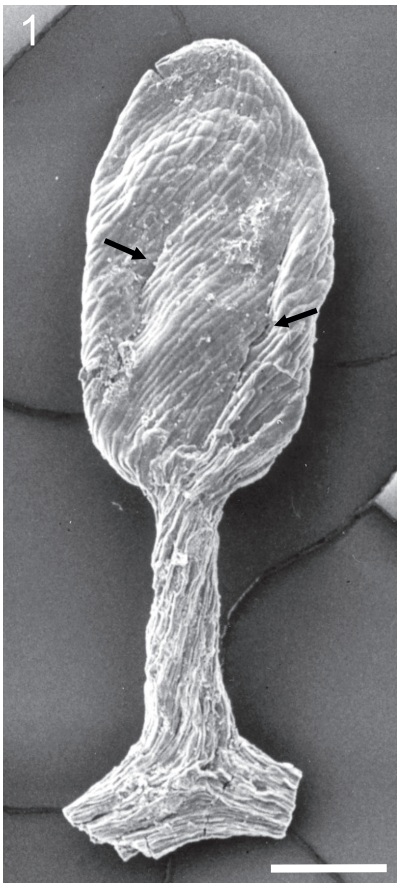
1

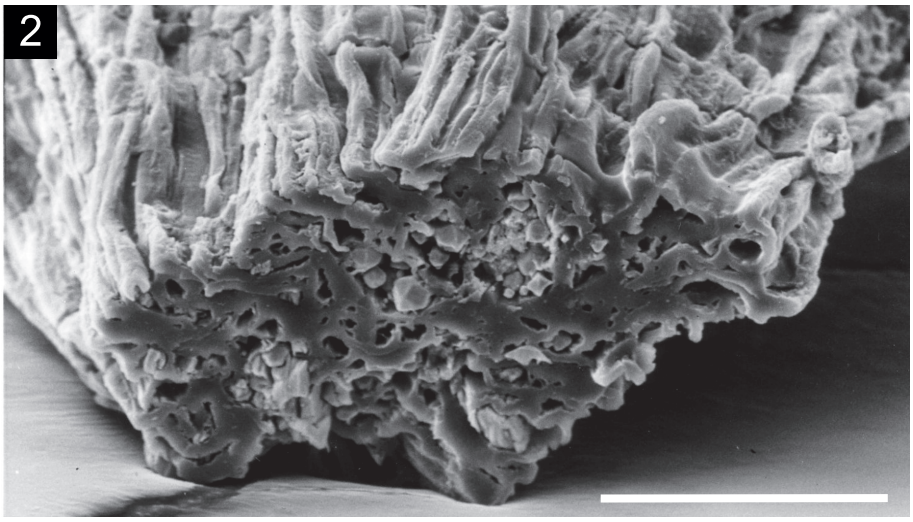
2

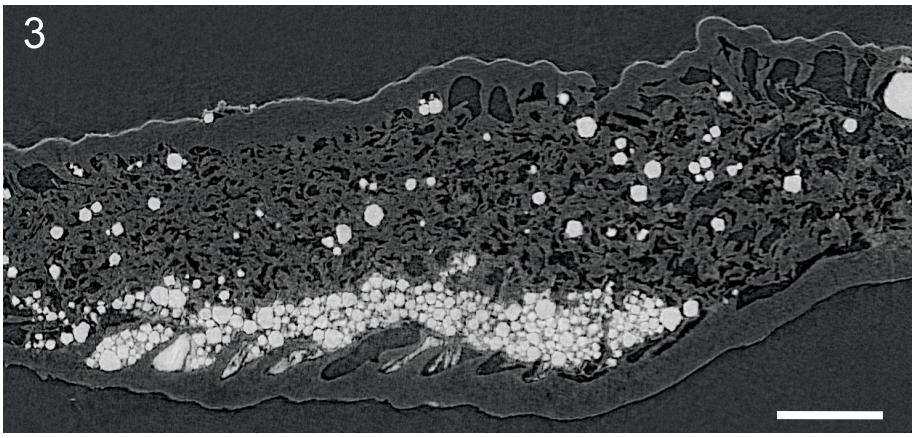
3


4

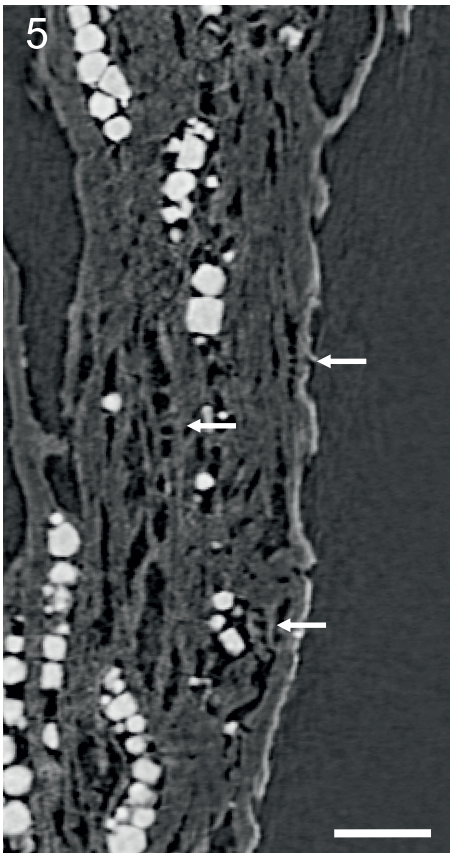
5


6

PLATE 4

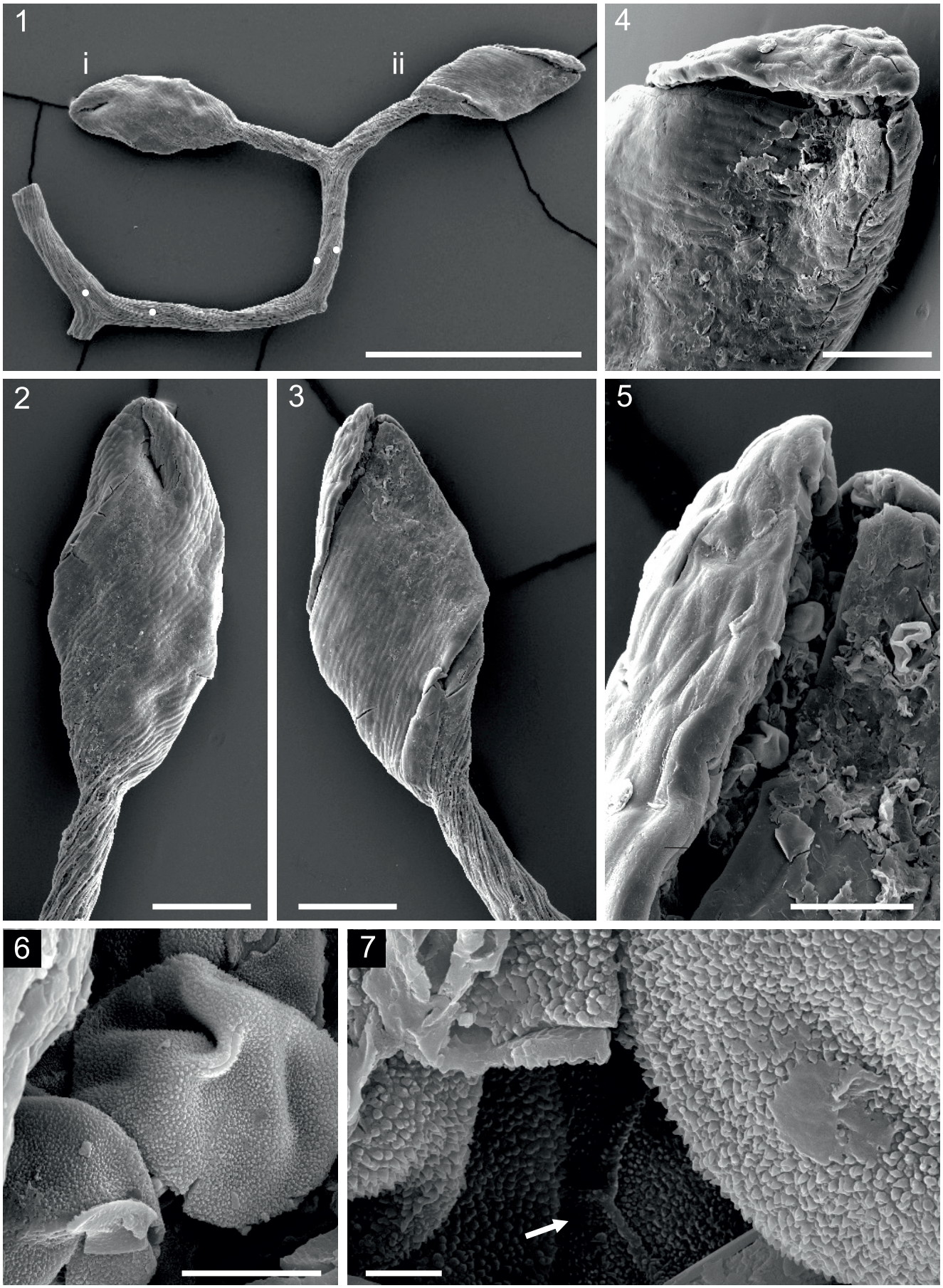

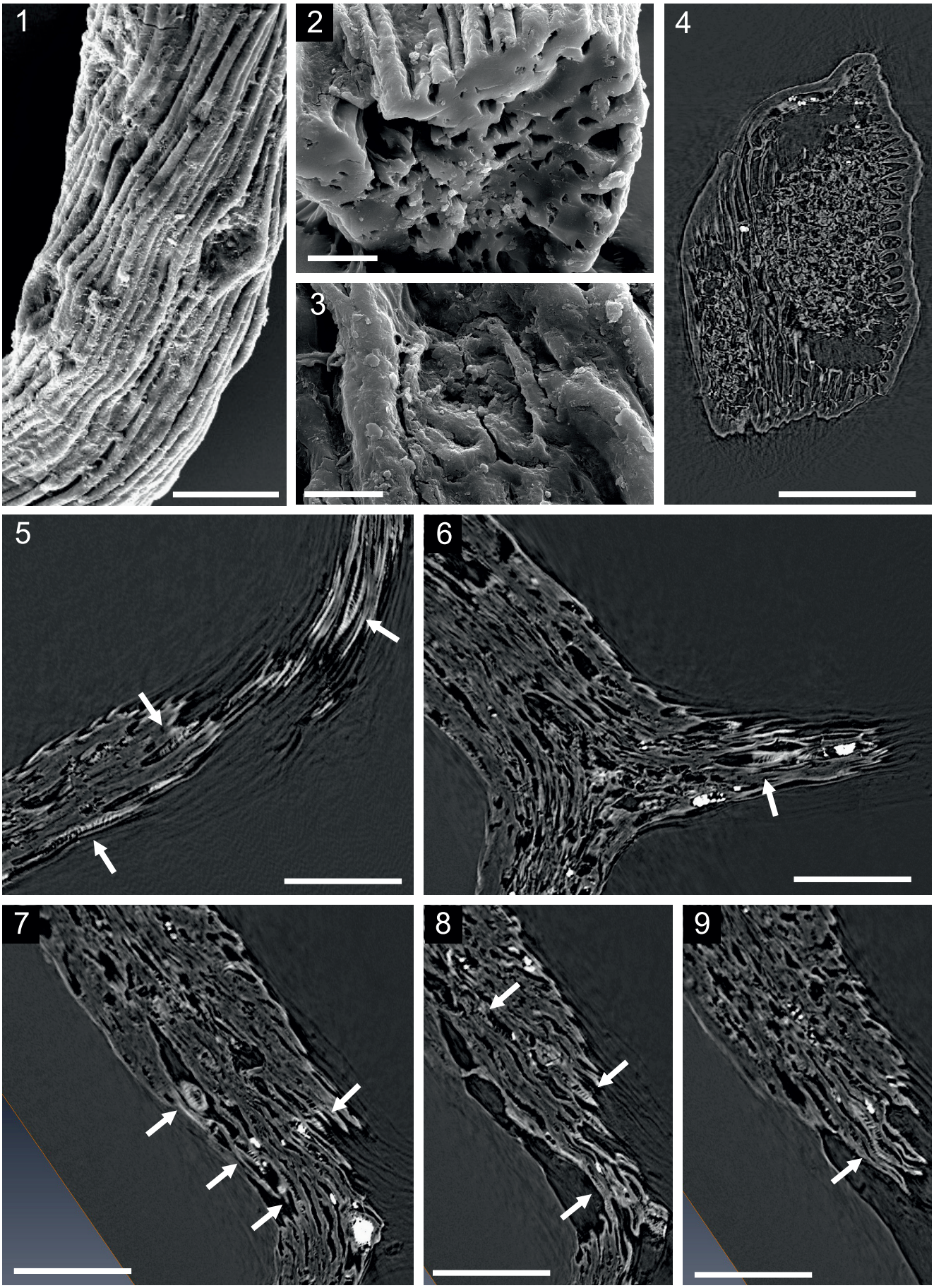
1
2
3
4
5
6
7
8
9

PLATE 6

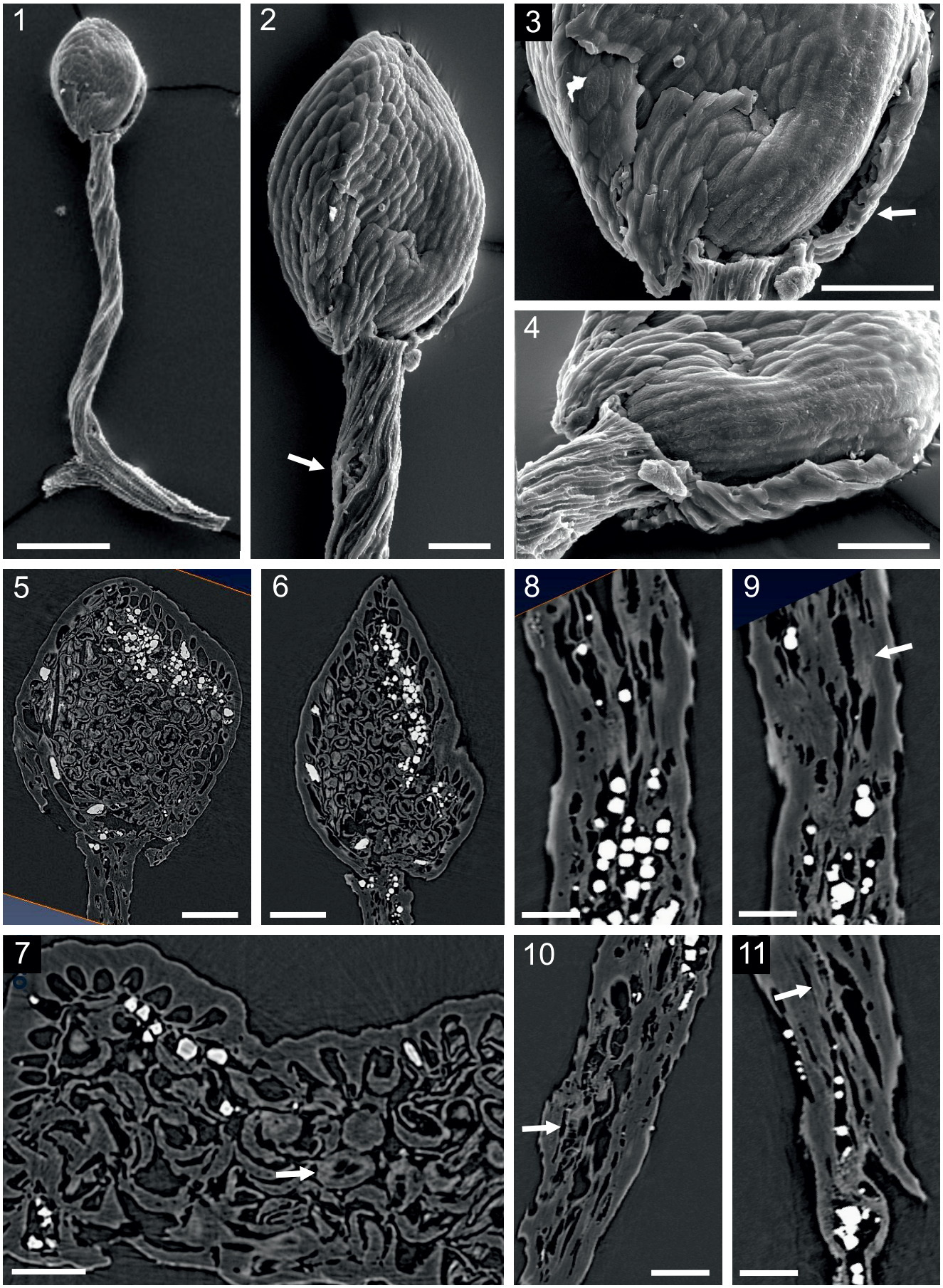

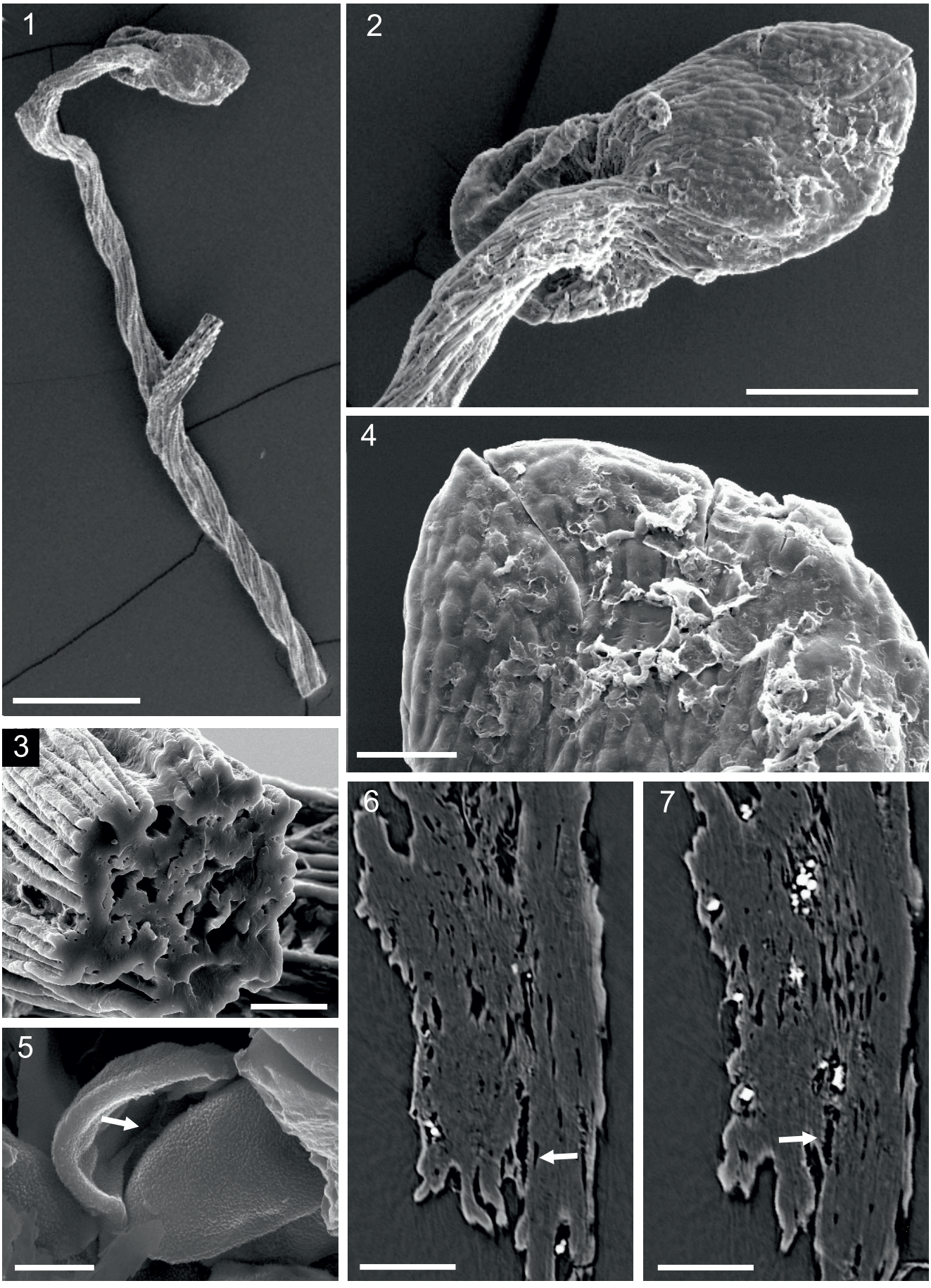
1
2
3
4
5
6
7